J. Cosmet. Sci., **70,** 299–312 (November/December 2019)

Effect of Palmitic Acid Conjugation on Physicochemical Properties of Peptide KTTKS: A Preformulation Study

SEYEDEH MARYAM MORTAZAVI, FARZAD KOBARFARD, HOWARD I. MAIBACH, and HAMID REZA MOGHIMI,
Department of Pharmaceutics and Nanotechnology, School of Pharmacy, Shahid Beheshti University of Medical Sciences, Tehran, Iran, 1991953381 (S.M.M., H.R.M.), Department of Medicinal Chemistry, School of Pharmacy, Shahid Beheshti University of Medical Sciences, Tehran, Iran, 1991953381 (F.K.), Department of Dermatology, School of Medicine, University of California, San Francisco, California, 94115 (H.I.M.), Protein Technology Research Center, Shahid Beheshti University of Medical Sciences, Tehran, Iran, 1991953381 (H.R.M.)

Accepted for publication September 21, 2019.

Synopsis

Lys–Thr–Thr–Lys–Ser (KTTKS) minimally crosses the skin because of hydrophilicity; therefore, its palmitoyl derivative, palmitoyl-KTTKS (Pal-KTTKS), is used in cosmetic products. In spite of this, there is insufficient information on its physicochemical properties and the effects of palmitoylation on such properties. The aim of this study was to investigate these properties. Such information would help appropriate formulation development. KTTKS and Pal-KTTKS were synthesized and characterized for ultra violet (UV) absorption, structure [X-ray diffraction (XRD)], morphology (electron microscopy), birefringence (polarized light microscopy), partitioning, solubility, thermal behavior (melting, thermogravimetric analysis, and differential scanning calorimetry), surface activity, critical micelle concentration (CMC, by tensiometry), and stability. KTTKS and Pal-KTTKS decomposed at about 154 and 150°C, respectively, and did not show a melting point before decomposition. The maximum UV absorbance of peptides was less than 200 nm. Both peptides showed birefringence, irregular flake morphologies, and hygroscopicity. KTTKS was freely soluble in water at room temperature ($\log P = -1.6 \pm 0.15$), indicating its hydrophilic nature. logP of Pal-KTTKS was calculated to be about 3.7, indicating a lipophilic compound. Pal-KTTKS showed surface activity with a CMC value of 0.024 ± 0.004 mM (19.25 ± 2.9 mg/L), whereas KTTKS did not show such surface activity. Palmitoylation demonstrated sharp peaks in the XRD pattern of KTTKS. KTTKS and Pal-KTTKS differ mainly in terms of chemical properties and show some similarity in physical properties. These results can be used for formulation developments.

INTRODUCTION

Skin aging prevention is an attractive issue in the cosmetic industry. Antiaging products include retinoids, alpha hydroxy acids, moisturizers, antioxidants (such as *L*-ascorbic acid, niacinamide, α-tocopherol, and ubiquinone), and peptides (1).

Address all correspondence to Hamid Reza Moghimi at hrmoghimi@sbmu.ac.ir and hrmoghimi@yahoo.com.

Purchased for the exclusive use of nofirst nolast (unknown)
From: SCC Media Library & Resource Center (library.scconline.org)

Based on their mechanism of action, topical peptides are classified into four categories: signal peptides, enzyme-inhibitor peptides, neurotransmitter-affecting peptides, and carrier peptides (1–4). Lys–Thr–Thr–Lys–Ser (KTTKS) (see Figure 1) is a signal peptide discovered by Katayama et al. in 1993. They demonstrated that extracellular matrix biosynthesis in human fetal lung fibroblasts was stimulated by KTTKS as a subfragment from C-peptides of type I procollagen, which is able to increase dermal remodeling (5).

Despite its high antiaging potential, this peptide minimally penetrates the skin. One strategy used to overcome this problem is conjugation to a lipophilic compound such as palmitic acid (a long-chain fatty acid containing 16 carbon atoms) (6). Palmitoyl-KTTKS (Pal-KTTKS) (see Figure 1) (brand name Matrixyl™, Sederma Inc., Le Perray-en-Yvelines, France) is available on the global market in antiaging formulations. Pal-KTTKS demonstrated improved effects on reduction of skin wrinkles in a 12-week, double-blind, placebo-controlled, clinical study on photoaged human facial skin (7). Fu et al. (8) demonstrated that niacinamide/Pal-KTTKS/retinyl propionate products had greater effect on improvement of wrinkle appearance than a 0.02% tretinoin product. Unfortunately, only few preformulation studies exist on them. Lack of information about physicochemical properties of these compounds leads to difficulty in their formulation.

Here, KTTKS and Pal-KTTKS were synthesized, and after confirmation by mass spectroscopy, physicochemical properties of both peptides and, therefore, the effects of covalent attachment of palmitic acid on KTTKS properties were investigated. To achieve these goals, ultra violet (UV) absorption ability, structure, morphology, birefringence, thermal

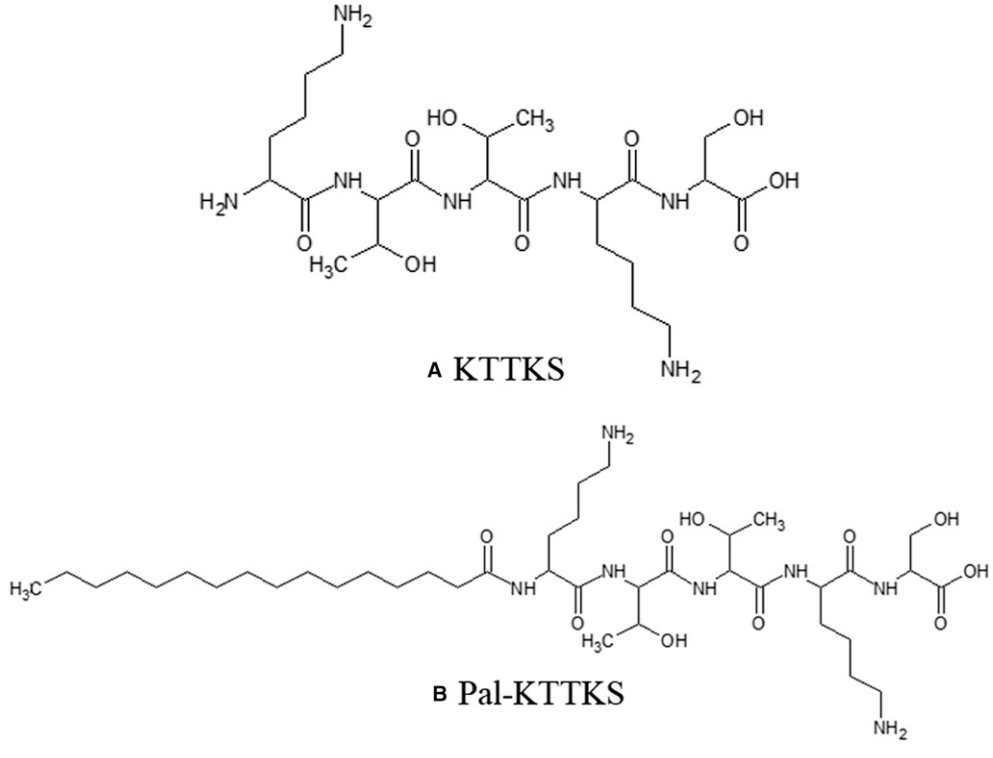

Figure 1. Chemical structure of KTTKS (A) and Pal-KTTKS (B).

Purchased for the exclusive use of nofirst nolast (unknown)
From: SCC Media Library & Resource Center (library.scconline.org)

behavior, aqueous solubility, partition coefficient, surface activity, critical micelle concentration (CMC), and aqueous stabilities were evaluated. The results should be useful for formulation development and also will provide information on palmitic acid conjugation of peptides, possibly useful for peptides other than KTTKS.

MATERIAL AND METHOD

MATERIALS

2-chlorotrityl chloride resin (loading capacity of 1.2 mmol/g), Fmoc-Ser(tBu)-OH, Fmoc-Thr(tBu)-OH, Fmoc-Lys(Boc)-OH, and 2-(7Aza-1H-benzotriazol-1-yl)-1,1,3,3-tetramethyluronium hexafluorophosphate (HATU) were provided by GL Biochem (Shanghai, China). Trifluoroacetic acid and piperidine were obtained from Exir GmbH (Wien, Austria). Ninhydrin was purchased from BDH Chemicals (Lutterworth, England). Isopropyl alcohol was supplied by ChemLab (Zedelgem, Belgium). Other solvents and reagents applied in the peptide synthesis process were purchased from Sigma-Aldrich (Dorset, United Kingdom) or Merck (Gernsheim, Germany). All materials were used without further purification.

METHODS

Peptide synthesis and characterization. KTTKS and Pal-KTTKS were synthesized by solid-phase peptide synthesis (SPPS) using the standard fluorenylmethyloxycarbonyl (Fmoc) strategy in a manual glass reaction vessel (9). The 2-chlorotrityl chloride resin was applied as an insoluble support, and to protect side chain reaction during the process, amino acids containing tert-butyloxycarbonyl (Boc) or tert-butyl side-chain protecting groups were used. After synthesis, confirmation of peptide integrity was accomplished by mass spectroscopy using an Agilent 6410 Triple Quad LC/MS (Agilent, Santa Clara, CA) with an electrospray ionization interface.

Determination of UV absorbance. Aqueous solutions of KTTKS and Pal-KTTKS were prepared individually. First, UV absorbance was set to zero with deionized water, and the solvent of peptide solution was used as the blank. UV absorbance of solutions was then measured over the wavelength range of 190–400 nm by a Cecil 2021 UV-Visible spectrophotometer (Cecil Instrument Services, Cambridge, United Kingdom) using a quartz cuvette with a 1-cm path length.

Evaluation of particle morphology by SEM. The morphology of KTTKS and Pal-KTTKS was analyzed by SU3500 scanning electron microscopy (Hitachi Ltd., Tokyo, Japan) at an accelerating voltage of 15 kV. Peptide powders were mounted on a stub of metal with adhesive, coated with gold, and then analyzed by SEM.

Evaluation of birefringence under polarized light microscopy. Birefringence was examined using a CETI Magnum binocular compound microscope (Medline Scientific, Oxford, United Kingdom) with a total magnification of 100×. The glass slide of each peptide powder was prepared and observed under cross-polarized light at ambient temperature.

Structure evaluation by X-ray diffraction (XRD). XRD patterns of KTTKS, Pal-KTTKS, and palmitic acid were measured using an X-ray diffractometer (X'Pert Pro MPD,

Purchased for the exclusive use of nofirst nolast (unknown)
From: SCC Media Library & Resource Center (library.scconline.org)

Panalytical B.V, Almelo,The Netherlands) at laboratory temperature (25°C) under the following conditions: voltage of 40 kV, current of 40 mA, and scan range of 1–80 2θ using Cu Kα radiation.

Partitioning and solubility investigation. The *n*-octanol/water partition coefficient (P_w^o) was obtained using the shake flask method for KTTKS and partition coefficient and solubility of Pal-KTTKS were computed using ACD/ChemSketch (ACD/Labs, Toronto, Canada) and ALOGPS (VCC-LAB, Munich, Germany) programs (10–12).

In the shake flask method, *n*-octanol and distilled water were mutually saturated with each other for 24 h before use. KTTKS was dissolved in water presaturated with *n*-octanol at a concentration of 200 µg/mL. In the following, *n*-octanol, presaturated with water, was added to the glass vials containing the aqueous solution of peptide. The glass vials were mixed by vortex for 2 min and then placed on an orbital shaker for 1 h to achieve equilibration. To separate the phases, contents of the glass vials were transferred to a separation funnel and left without shaking for 0.5 h. The phases were separated and concentrations of peptide in the aqueous phase were measured by LC–MS, as described in the Peptide assay by LC-MS section. The *n*-octanol/water partition coefficient was then calculated using equation 1 (13):

$$\log P_w^o = \log \frac{C_o}{C_w}, \tag{1}$$

where C_o and C_w are the concentrations of peptide in *n*-octanol and water after equilibration, respectively. The experiment was performed in triplicate.

Aqueous solubility of KTTKS was estimated by adding increasing amounts of peptide to a certain volume of distilled water at room temperature.

Surface tension measurement of peptide solutions. Surface tensions of aqueous solutions of KTTKS and Pal-KTTKS (prepared individually with concentrations of 100 µg/mL) as well as deionized water were measured by a K100 Force tensiometer (Krüss GmbH, Hamburg, Germany) using the Du Noüy ring method at room temperature. In addition, the surface tensions of both peptides and also deionized water were calculated by the ACD/ChemSketch freeware software. This software calculates the surface tension via molar volume and parachor (14).

Determination of CMC. Aqueous solution of Pal-KTTKS was prepared using deionized water. The CMC value was then measured fully automatically by the K100 Force tensiometer (with one micro dispenser) using the Du Noüy ring method at room temperature. The measurement was repeated three times.

Thermal behavior. Thermal behaviors of peptides were evaluated by IA9000 series capillary melting apparatus (Cole-Parmer Instrument, Vernon Hills, IL), TGA-50, and DSC-60 (Shimadzu, Kyoto, Japan) thermal analysis systems. The melting point apparatus was used to determine the melting points. The capillary tube was packed by gently pressing the open end into the peptide powders. The bottom of the capillary tube was then tapped on a hard surface so that the peptide powders packed down into the bottom of the capillary tube. The capillary tubes containing the peptide powder were inserted into the apparatus holder. Ramp rate of 5°C/min was adjusted. The peptide powders were then examined through the magnifying glass of the apparatus, and changes in the powder bed were recorded during the temperature rise.

Purchased for the exclusive use of nofirst nolast (unknown)
From: SCC Media Library & Resource Center (library.scconline.org)

Thermogravimetric analysis (TGA) was conducted to determine peptide decomposition. About 4–5 mg of peptide powder was weighed into an open TGA aluminum pan and heated from ambient temperature to 595°C at a heating rate of 10°C/min under a nitrogen atmosphere. The experiment was performed in triplicate.

Differential scanning calorimetry (DSC) was performed for determination of peptides' thermal characteristics. First, using indium as a standard, the DSC instrument was calibrated. About 3–5 mg of peptide powder was then put into the DSC aluminum pan. The pan was sealed and thermal behavior studied at a heating rate of 10°C/min under a nitrogen atmosphere. The experiment was performed in triplicate. In another experiment, a cycled heating method was used. First, the pans containing KTTKS or Pal-KTTKS were individually heated to 100°C, and after cooling, the same pans were reheated to 165°C.

Cycled TGA experiments were also used here to interpret DSC data. In this experiment, the pan containing peptide was heated to 100°C at a heating rate of 5°C/min and then cooled to room temperature. The same pan was then heated again to 100°C at the same heating rate. Thermogram was then analyzed for any weight change.

Stability studies. An aqueous solution of KTTKS was prepared at a concentration of 100 µg/mL and aliquoted into glass vials. The vials were then studied separately at 32°C in a water bath for 48 h. Peptide concentration was then measured by LC–MS, as described in the later section. The experiment was performed in triplicate.

Peptide assay by LC-MS. The concentration of KTTKS was quantified by a selected ion chromatogram method using an Agilent 6410 Triple Quad LC/MS system under the following conditions: Capital C8-Optimal column (250 × 4.6 mm, i.e., 5 µm), isocratic elution, mobile phase of acetonitrile (40%): 20 mM ammonium acetate solution containing 0.05% acetic acid glacial (60%), nitrogen dry gas at a temperature of 300°C and pressure of 25 psi, injection volume of 25 µL, and flow rate of 0.6 mL/min. A mass to charge (m/z) ratio of 564.2 was used to detect KTTKS.

Statistical analysis. SPSS Statistics software version 21.0 (IBM, Armonk, NY) was used for data analysis. Independent sample t-test was used to determine the statistical significance of data. Differences were considered to be significant for values of $p < 0.05$.

RESULTS

PEPTIDE SYNTHESIS AND CHARACTERIZATION

Peptides, which were synthesized by SPPS using the Fmoc methodology, were confirmed by mass spectrometry. The singly charged molecular ion $[M+H]^+$ at an m/z of 564.2 and the doubly charged molecular ion $[M+H]^{2+}$ at an m/z of 282.7 confirmed the synthesis of KTTKS. In the case of Pal-KTTKS, $[M+H]^+$ at an m/z of 802.3 and $[M+H]^{2+}$ at an m/z of 401.7 confirmed the synthesis of Pal-KTTKS.

DETERMINATION OF UV ABSORBANCE

Finding an appropriate assay method to quantify a drug candidate is an important step in preformulation studies. UV spectroscopy is a simple and widely available analytical method.

Purchased for the exclusive use of nofirst nolast (unknown)
From: SCC Media Library & Resource Center (library.scconline.org)

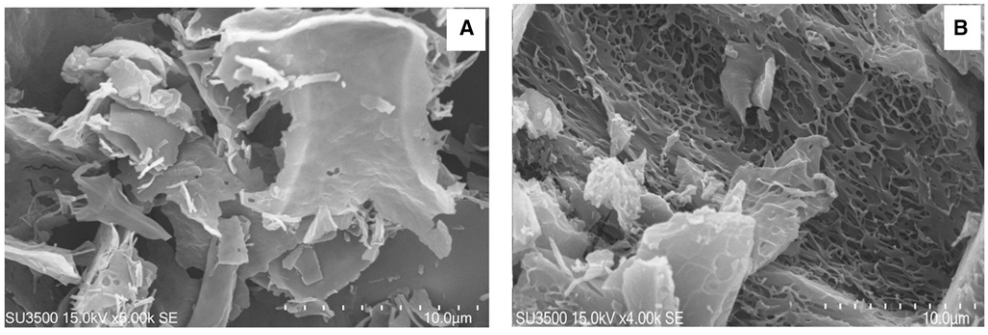

Figure 2. SEM images of peptides: (A) KTTKS and (B) Pal-KTTKS.

Hence, the UV absorbance ability of KTTKS and Pal-KTTKS was evaluated. The λ_{max} (wavelength of maximum) of KTTKS and Pal-KTTKS was found to be 193 and 195 nm, respectively.

EVALUATION OF PARTICLE MORPHOLOGY BY SEM

Scanning electron microscope images of KTTKS and Pal-KTTKS are illustrated in Figure 2. Generally, there is minimal difference between the morphology of KTTKS and Pal-KTTKS particles. Both peptides showed irregular flake morphologies with a wide particle size distribution.

EVALUATIONS OF BIREFRINGENCE UNDER POLARIZED LIGHT MICROSCOPY

Polarizing light microscopy images of KTTKS and Pal-KTTKS are presented in Figure 3. As clearly seen, both peptides show birefringence under cross-polarized light, indicating their anisotropic structure. Therefore, it could be definitely said that KTTKS and Pal-KTTKS are not amorphous and do not possess the isotropic cubic crystalline lattice structure.

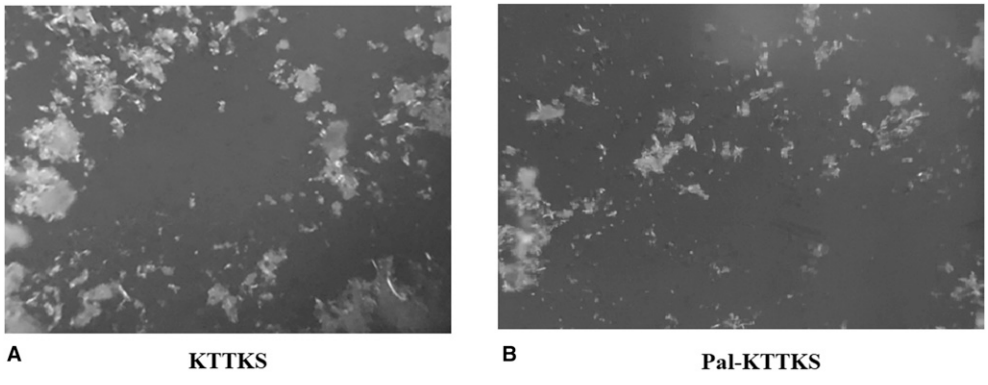

Figure 3. Polarizing light microscopy images of KTTKS (A) and Pal-KTTKS (B).

Purchased for the exclusive use of nofirst nolast (unknown)
From: SCC Media Library & Resource Center (library.scconline.org)

STRUCTURE EVALUATION BY XRD

XRD was applied to understand the solid-state form of peptides, which is possibly the most important state in developing a drug candidate into a drug product (15). Patterns of reflection intensity versus 2θ are shown in Figure 4. As seen, the XRD pattern of palmitic acid displayed an ordered structure. Peaks with the highest intensities are presented in Table I. The XRD pattern of KTTKS shows two peaks in a wide range of Bragg's angles: one broad peak at 2θ = 19.5 with d-spacing (repeat distance) of 8.7 Å and another at 2θ = 10.1 with d-spacing of 4.5 Å (Figure 4). After peptide modification with palmitic acid (Pal-KTTKS), in addition to two peaks at 2θ = 10.6 (d-spacing = 8.3 Å) and 2θ = 19.1 (d-spacing = 4.6 Å), which are close to that of KTTKS, a peak at 2θ = 21.3 (d-spacing = 4.1 Å) appears. In addition, three other peaks appear in the small angle area: a sharp peak at 2θ = 2.0 with d-spacing of 44.2 Å, a peak at 2θ = 6.5 with d-spacing of 13.6 Å, and a peak at 2θ = 9.5 with d-spacing of 9.34 Å, indicating the presence of a long-range order in Pal-KTTKS.

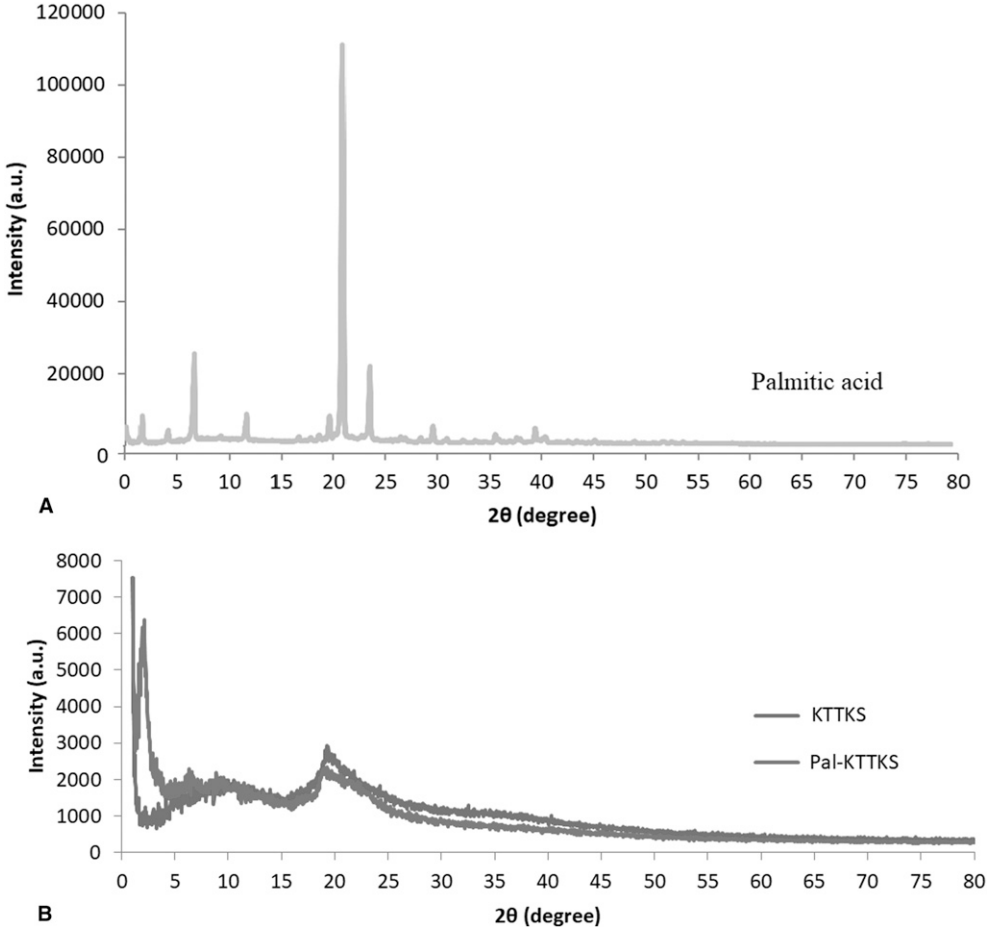

Figure 4. XRD pattern of palmitic acid (A) and comparison of XRD patterns of KTTKS and Pal-KTTKS (B) at ambient temperature.

Purchased for the exclusive use of nofirst nolast (unknown)
From: SCC Media Library & Resource Center (library.scconline.org)

Table I
Summary of XRD Patterns of Palmitic Acid at Ambient Temperature

2θ (degree)	Repeat distance (Å)	Relative intensity (%)
2.6	34.6	6.2
7.5	11.7	17.5
20.5	4.3	5.9
21.7	4.1	100
24.3	3.7	18.6
30.3	2.9	4.4

PARTITIONING AND SOLUBILITY

Partition coefficient is a determining property which affects the permeation of a permeant across the skin. The experimental logP value of KTTKS, obtained through the shake flask method, was -1.6 ± 0.15.

We could not determine logP of Pal-KTTKS experimentally because this molecule apparently self-aggregates in *n*-octanol–saturated water even at low concentrations (as low as 25 μg/mL). The same problem occurred when n-hexadecane was used as the oily phase. Lower concentrations were not used because of detection limitations. In such situations, formulators can use different software, such as ACD/ChemSketch, to calculate logP. The calculated logP (clogP) of Pal-KTTKS obtained here by this software was found to be 3.7 (11). Therefore, it could be concluded that the peptide conjugate Pal-KTTKS is much more lipophilic than KTTKS (logP = −1.6) and might be a better candidate for skin permeation than KTTKS. Such a compound might even get trapped in the lipid domain of the stratum corneum. Such a lipophilic molecule is expected to be soluble in lipophilic vehicles, such as ointments or oily phase of o/w and w/o emulsions and creams.

KTTKS aqueous solubility was estimated to exceed 220 mg/mL, which is considered as freely soluble. However, we were unable to determine the solubility of Pal-KTTKS because of its complex behavior in aqueous systems possibly due to its self-aggregation and assembly. Solubility estimation by ALOGPS revealed an aqueous solubility of 0.02 mM (0.016 mg/mL) for Pal-KTTKS, in good agreement with CMC value obtained by the ring method, as discussed later.

SURFACE TENSION MEASUREMENT OF PEPTIDE SOLUTIONS

Theoretical and experimental surface tensions of both peptides as well as deionized water obtained by ACD-ChemSketch software and the ring method, respectively, are provided in Table II. The experimental surface tension of KTTKS aqueous solution was

Table II
Theoretical and Experimental Surface Tensions of Deionized Water, KTTKS, and Pal-KTTKS

	Theoretical surface tension (mN/m)	Experimental surface tension (mN/m) ($n = 3$)
Deionized water	72.2 ± 3	70.8 ± 0.05
KTTKS	63.1 ± 3	69.0 ± 2.7
Pal-KTTKS	50.1 ± 3	50.3 ± 0.4

Purchased for the exclusive use of nofirst nolast (unknown)
From: SCC Media Library & Resource Center (library.scconline.org)

69.0 ± 2.7 mN/m, which is almost identical to the surface tension of water (70.8 ± 0.05 mN/m) ($p > 0.05$, independent sample t-test). For aqueous solution of Pal-KTTKS, the surface tension was reduced significantly to 50.3 ± 0.4 mN/m ($p < 0.05$, independent sample t-test), indicating that this peptide possesses surface activity. These data agree with the surface tension obtained using software, which was 50.1 ± 3 mN/m.

DETERMINATION OF CMC

Because of surface activity, the CMC value of Pal-KTTKS aqueous solution was determined by the ring method and found to be 0.024 ± 0.004 mM; as will be discussed later, such activity is expected based on the amphiphilic behavior of Pal-KTTKS.

THERMAL BEHAVIOR

Thermal behavior and stability of peptides are important issues during formulation, storage, and permeation studies of these molecules. Hence, thermal behaviors of KTTKS and Pal-KTTKS were investigated here. The results obtained from the melting apparatus demonstrated that both peptides decomposed before melting. Their decomposition temperatures were observed at 154 and 150°C for KTTKS and Pal-KTTKS, respectively.

The TGA and the first derivative TGA thermograms of KTTKS and Pal-KTTKS are shown in Figure 5A and B and results summarized in Table III. There are three distinct weight loss areas in TGA thermograms for both peptides. Based on the results of the melting point apparatus, DSC (as explained in the following paragraph), and data obtained from the TGA analysis, it could be said that the first weight loss area in the TGA thermograms of KTTKS and Pal-KTTKS (25–150°C) could be probably attributed to evaporation of water, as explained later. The second and third weight loss areas (150–250 and 250–595°C), where more weight loss has occurred, are presumably relevant to peptide

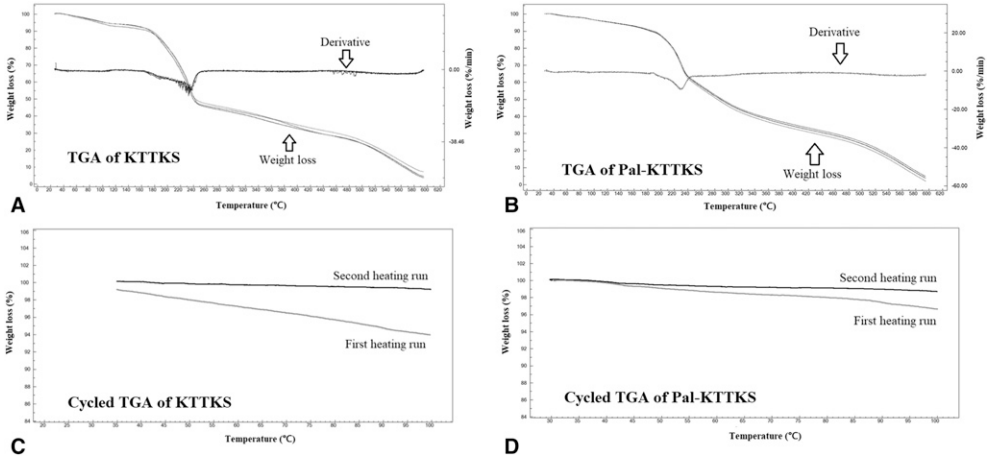

Figure 5. TGA thermograms and their first derivatives for KTTKS (A) and Pal-KTTKS (B) at a heating rate of 10°C/min over 25–595°C ($n = 3$), and also heating–cooling–heating cycle TGA thermograms of KTTKS (C) and Pal-KTTKS (D) at a heating rate of 5°C/min over 25–100°C.

Purchased for the exclusive use of nofirst nolast (unknown)
From: SCC Media Library & Resource Center (library.scconline.org)

Table III
Percent Weight Loss of Peptides and the Temperature of Maximum Weight Loss during TGA Study in the Range of 25–595°C

Peptide name	Weight loss (%) over three temperature ranges			Temperature of maximum weight loss (°C)
	25–150°C	150–250°C	250–595°C	
KTTKS	7.47 ± 0.84	45.34 ± 1.29	41.97 ± 1.03	233.92 ± 1.49
Pal-KTTKS	6.55 ± 0.99	33.61 ± 0.67	56.38 ± 0.67	229.26 ± 0.86

Data are represented as mean ± SD ($n = 3$).

decomposition. The temperature of maximum weight loss (≈230°C) obtained from the first derivative TGA thermograms is almost similar for both peptides (see Table III).

DSC thermograms of KTTKS and Pal-KTTKS are illustrated in Figure 6A. As seen, both peptides exhibit endothermic transitions with a peak of 59.8 ± 1.3°C ($T_{1\ KTTKS}$) for KTTKS and 50.6 ± 4.4°C ($T_{1\ Pal\text{-}KTTKS}$) for Pal-KTTKS. Given the results obtained from the melting point studies, which showed that peptides did not show any sign of melting, these endothermic transitions could not be attributed to the melting of peptides and were assumed here to be water-related intrinsic structural rearrangement, polymorphism, or evaporation, as discussed later. KTTKS has another endothermic peak with low enthalpy ($T_{2\ KTTKS}$) (see Figure 6A). A third endothermic transition ($T_{3\ KTTKS}$) starts at 152.1 ± 3.9°C in the thermogram of KTTKS. This endotherm is in good agreement with the result of decomposition obtained from melting point studies (154°C). For Pal-KTTKS, the second endothermic transition ($T_{2\ Pal\text{-}KTTKS}$), starting at 142.7 ± 0.9°C, could also be attributed to the first decomposition of the peptide conjugate as observed in melting point studies (150°C). Visual observations of the DSC pan after removal revealed sever changes in the peptide appearance (change in color and texture). These changes might be considered as signs of peptide decomposition.

To ascertain the nature of $T_{1\ KTTKS}$ and $T_{1\ Pal\text{-}KTTKS}$, cycled DSC was performed. Cycled DSC experiment indicated that $T_{1\ KTTKS}$ and $T_{1\ Pal\text{-}KTTKS}$ disappeared in the second heating run, whereas $T_{2\ KTTKS}$, $T_{3\ KTTKS}$, and $T_{2\ Pal\text{-}KTTKS}$ remained unchanged (see Figure 6B). These results might show that $T_{1\ KTTKS}$ and $T_{1\ Pal\text{-}KTTKS}$ are related to water evaporation from peptides, as discussed later.

To ensure the relationship of $T_{1\ KTTKS}$ and $T_{1\ Pal\text{-}KTTKS}$ to water evaporation, a cycled TGA experiment was performed here. As shown in Figure 5C and D, TGA weight losses for the first heating runs are 5.9% and 3.3% for KTTKS and Pal-KTTKS, respectively.

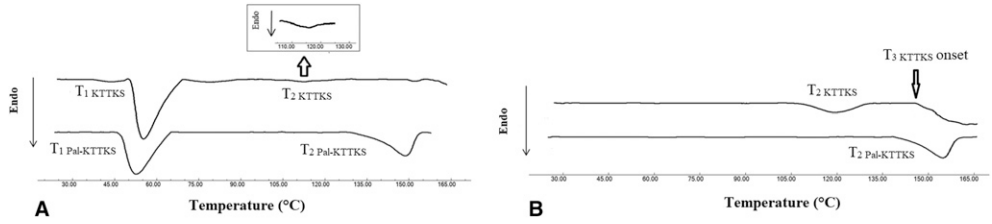

Figure 6. (A) Sample DSC thermograms of KTTKS and Pal-KTTKS at a heating rate of 10°C/min over 25–165°C and (B) DSC thermograms of preheated–cooled KTTKS and Pal-KTTKS samples at a heating rate of 10°C/min over 25–165°C (see text for more explanation).

Purchased for the exclusive use of nofirst nolast (unknown)
From: SCC Media Library & Resource Center (library.scconline.org)

In the second heating runs, weight losses were less than 1% for both peptides. After both heating processes in TGA, the pans containing peptides were inspected visually; there were no macroscopic changes in the appearance of peptide powders. In agreement with the present results, some researchers (16) showed that a DSC transition of around 63.1°C in a lyophilized synthetic trapezoid-inspired peptide fragment disappeared in the second DSC heating run. It was concluded by investigators to be due to the presence of bound water and subsequent water loss in the second run.

STABILITY STUDIES

Ensuring the stability of permeants during the skin permeation experiment is crucial. The concentration of KTTKS solution was 100 μg/mL at the beginning of the stability study. After 48 h, the concentration of KTTKS solution reached 99.3 ± 1.7 μg/mL. Thus, it could be concluded that KTTKS remains stable at 32°C at least for 48 h. Therefore, there is no concern about the instability of this permeant during the skin permeation studies for at least 48 h.

DISCUSSION

KTTKS and its derivative are popular in the cosmetic industry because of their anti-wrinkle properties, but many of their physicochemical properties remain unknown. This study is an attempt to define the physicochemical properties of these peptides and to investigate the effects of covalent attachment of a fatty acid on peptide properties.

In the case of UV absorbance, λ_{max} of both peptides was at less than 200 nm. KTTKS and Pal-KTTKS have no aromatic amino acids in their structure, and the UV absorbance of them is due to the peptide bonds. The photons are absorbed by peptide bond at the maximum wavelength of below 210 nm (17). Note that the wavelengths below 200 nm belong to vacuum UV (18). The UV radiation is forcefully absorbed by atmospheric oxygen in the vacuum UV range (19). Therefore, a free oxygen environment is required to accurately assay KTTKS and Pal-KTTKS if UV spectroscopy at the maximum wavelength is to be used. Because KTTKS and Pal-KTTKS possess a broad absorption peak, it might be said that it is possible to measure the absorption at the longer wavelength, e.g., at 205 nm, but we noted that at this wavelength, the UV radiation is absorbed by many compounds used in buffers (20), which are mainly applied in skin permeation studies.

In X-ray studies, both peptides showed a broad peak (hump) at around $2\theta = 19°$ (see Figure 4), which was absent in palmitic acid. Such a broad peak at a wide angle region, which has also been reported for other peptides (21), might indicate that these peptides contain either some amorphous structures or some disordered crystalline structures. Both peptides also show peaks at $2\theta \leq 10$ that indicate some long-range orders. The presence of some degrees of orders in the structure was also confirmed by showing birefringence in the cross-polarized light. The presence of new peaks in the XRD pattern of Pal-KTTKS, which is not present in the pattern of KTTKS, means that the structures of these peptides are not the same; therefore, some possible changes in the physicochemical properties of peptides, such as solubility, dissolution rate, and flowability, are expected and should be considered by formulators.

Purchased for the exclusive use of nofirst nolast (unknown)
From: SCC Media Library & Resource Center (library.scconline.org)

Palmitic acid molecules form dimers because of OH….O hydrogen bonds and these dimers pack into bilayers (22,23). Palmitic acid has a small polar head group (–COOH). Changing the head group to bulky KTTKS probably imposes some degree of disorder into the structure. Besides this, the molecules become longer with higher d-spacing: 34.6 Å for palmitic acid versus 44.2 Å for Pal-KTTKS. Pal-KTTKS also shows a higher d-spacing than KTTKS that are definitely due to the presence of long chain (C16) in the structure.

Based on the results of partitioning and solubility tests, KTTKS has a highly hydrophilic nature (logP < 0 and high water solubility). Because higher lipophilicity is required for good permeation through the skin (logP 0–3), KTTKS, like many other peptides such as Ala–Ala–Pro–Val (24), tetragastrin (25), and TRH (26), is not a good candidate for skin delivery. The results of the *in vitro* skin permeation study of KTTKS, which showed KTTKS did not permeate across the skin (27), is in good agreement with the present finding.

KTTKS is a pentapeptide without a hydrophobic tail, but Pal-KTTKS has a 16-carbon chain (palmitic acid) as the hydrophobic tail, so Pal-KTTKS is a peptide amphiphile. The peptide amphiphiles are capable of forming a diversity of aggregates, such as micelles, cylindrical fibrils, sheets, and vesicles (28). Here, the results of tensiometry indicate that Pal-KTTKS has surface activity and reduces the surface tension of water to 50.3 ± 0.4 mN/m. The CMC of Pal-KTTKS in water was also determined by the ring method and found to be 0.024 ± 0.004 mM. There are no reports on the CMC value of Pal-KTTKS in aqueous solutions using the ring method. This CMC value resembles polysorbate 80 (0.02–0.03 mM) (29), which is structurally similar to Pal-KTTKS. The CMC value could be considered as the solubility of the individual molecules with surface activity because above this concentration, the molecules are not dissolved in the monomeric forms and aggregate as micelles (30). As said, this value for Pal-KTTKS was 0.024 ± 0.004 mM or 19.25 ± 2.9 mg/L; thus, considering only individual molecules, it could be said this peptide amphiphile is practically insoluble in water.

Cycled DSC and TGA results show that both peptide powders are hygroscopic. The hygroscopic nature of some peptides, especially when present as porous lyophilized powders, is a well-known property. On the other hand, it has been argued that peptides containing charged amino acids (such as arginine, aspartic acid, glutamic acid, histidine, and lysine) are hygroscopic (31). KTTKS and its derivative have two lysine amino acids, and therefore, it is possible that they absorb water. Hence, two water-related transitions ($T_{1\ KTTKS}$ and $T_{1\ Pal\text{-}KTTKS}$) in their DSC thermograms disappear on reheating, which is in agreement with weight losses observed in TGA thermograms.

Finally, as far as formulation is concerned, techniques such as UV, XRD, polarized light microscopy, SEM, and thermal analysis can be used to monitor changes during pharmaceutical processing, stability studies, and storage by the formulator. Some of these techniques, e.g., DSC, can be used to determine drug–excipients interactions. During pharmaceutical processing and storage, a formulator should be aware of the polymorphism and the possibility of change of a polymorphic form into another due to processing (such as mixing and heating) and storage. For example, if a formulator uses these substances in the suspension dosage form (the presence of solid particles in the formulation), the stability during storage can be monitored using XRD or polarized light microscopy, as described earlier. The same applications apply to the SEM morphologies. SEM and polarized light

Purchased for the exclusive use of nofirst nolast (unknown)
From: SCC Media Library & Resource Center (library.scconline.org)

represent crystal habits as well. In this regard, some habits such as needle-likes might provide some degrees of discomfort in topical applications and should be considered in the formulation and stability studies by the formulator.

CONCLUSION

Here, KTTKS and Pal-KTTKS were synthesized and the physicochemical properties of both peptides and, therefore, the effects of covalent attachment of palmitic acid on KTTKS properties were investigated. In short, these peptides showed birefringence, irregular morphology, wide particle size distribution, and no melting point before decomposition. In addition, KTTKS was very hydrophilic in nature, and its aqueous solution remains stable at 32°C for over 48 h. In terms of internal structure, Pal-KTTKS appeared more ordered than KTTKS. Micelle formation of Pal-KTTKS in water occurs at low concentrations. The results show that fatty acid attachment to KTTKS causes some changes in chemical properties (such as solubility and partition coefficient), whereas physical properties (such as morphology, thermal behavior, and birefringence) are not affected so much. These results can be used for formulation of these peptides for topical delivery or any other drug delivery system development. The effects of palmitic acid conjugation on KTTKS properties might be used for the preparation of palmitic acid derivatives on other peptides.

ACKNOWLEDGMENTS

This paper is a part of PhD thesis of Seyedeh Maryam Mortazavi at the School of Pharmacy, Shahid Beheshti University of Medical Sciences (SBMU), Tehran, Iran and was financially supported by SBMU.

REFERENCES

(1) M. Ramos-e-Silva, L. Celem, S. Ramos-e-Silva, and A. P. Fucci-da-Costa, Anti-aging cosmetics: facts and controversies, *Clin. Dermatol.*, **31**, 750–758 (2013).
(2) N. H. Abu Samah and C. M. Heard, Topically applied KTTKS: a review. *Int. J. Cosmet. Sci.*, **33**, 483–490 (2011).
(3) S. Schagen, Topical peptide treatments with effective anti-aging results, *Cosmetics*, **4**, 16 (2017).
(4) F. Gorouhi and H. I. Maibach, Role of topical peptides in preventing or treating aged skin, *Int. J. Cosmet. Sci.*, **31**, 327–345 (2009).
(5) K. Katayama, J. Armendariz-Borunda, R. Raghow, A. H. Kang, and J. M. Seyer, A pentapeptide from type I procollagen promotes extracellular matrix production, *J. Biol. Chem.*, **268**, 9941–9944 (1993).
(6) C. Lu, B. M. Kim, D. Lee, M. H. Lee, J. H. Kim, H. B. Pyo, and K. Y. Chai, Synthesis of lipoic acid-peptide conjugates and their effect on collagen and melanogenesis, *Eur. J. Med. Chem.*, **69**, 449–454 (2013).
(7) L. R. Robinson, N. C. Fitzgerald, D. G. Doughty, N. C. Dawes, C. A. Berge, and D. L. Bissett, Topical palmitoyl pentapeptide provides improvement in photoaged human facial skin, *Int. J. Cosmet. Sci.*, **27**, 155–160 (2005).
(8) J. J. Fu, G. G. Hillebrand, P. Raleigh, J. Li, M. J. Marmor, V. Bertucci, P. E. Grimes, S. H. Mandy, M. I. Perez, S. H. Weinkle, and J. R. Kaczvinsky, A randomized, controlled comparative study of the wrinkle reduction benefits of a cosmetic niacinamide/peptide/retinyl propionate product regimen vs. a prescription 0.02% tretinoin product regimen, *Br. J. Dermatol.*, **162**, 647–654 (2010).
(9) G. B. Fields and R. L. Noble, Solid phase peptide synthesis utilizing 9-fluorenylmethoxycarbonyl amino acids, *Int. J. Pept. Protein Res.*, **35**, 161–214 (1990).

Purchased for the exclusive use of nofirst nolast (unknown)
From: SCC Media Library & Resource Center (library.scconline.org)

(10) OECD, *Test No. 107: Partition Coefficient (n-octanol/water): Shake Flask Method*, OECD Publishing, Paris, France (1995).
(11) ACD/Labs, *Partition Coefficient Calculation with ACD/LogP*, Advanced Chemistry Development, Inc., 2019, accessed June 21, 2019, https://www.acdlabs.com/products/percepta/predictors/logp/.
(12) I. V. Tetko, J. Gasteiger, R. Todeschini, A. Mauri, D. Livingstone, P. Ertl, V. A. Palyulin, E. V. Radchenko, N. S. Zefirov, A. S. Makarenko, V. Y. Tanchuk, and V. V. Prokopenko, Virtual computational chemistry laboratory - design and description. *J. Comput. Aided Mol. Des.*, **19**, 453–463 (2005).
(13) S. Gaisford, "Pharmaceutical preformulation," in *Aulton's Pharmaceutics: The Design and Manufacture of Medicines*, 5th Ed., M. E. Aulton and K. M. G. Taylor. Eds. (Churchill Livingstone, London, 2018), pp. 391–392.
(14) ACDLabs, *ACD/ChemSketch.12.01 edn* (Advanced Chemistry Development, Inc., Toronto, 2009).
(15) S. Gaisford, "Pharmaceutical preformulation," in *Aulton's Pharmaceutics: The Design and Manufacture of Medicines*, M. Aulton and K. Taylor. Eds. (Churchill Livingstone, London, 2018), pp. 402.
(16) J. Dandurand, V. Samouillan, M. H. Lacoste-Ferre, C. Lacabanne, B. Bochicchio, and A. Pepe, Conformational and thermal characterization of a synthetic peptidic fragment inspired from human tropoelastin: signature of the amyloid fibers, *Pathol. Biol.*, **62**, 100–107 (2014).
(17) J. E. Noble and M. J. Bailey, Quantitation of protein, *Methods Enzymol.*, **463**, 73–95 (2009).
(18) A. R. Field, J. Fink, R. Dux, G. Fußmann, U. Wenzel, and U. Schumacher, A spatially scanning vacuum ultraviolet and visible range spectrometer for spectroscopy of tokamak plasmas in ASDEX-Upgrade, *Rev. Sci. Instrum.*, **66**, 5433–5441 (1996).
(19) B. B. Stephens, R. F. Keeling, and W. J. Paplawsky, Shipboard measurements of atmospheric oxygen using a vacuum-ultraviolet absorption technique, *Tellus B Chem. Phys. Meteorol.*, **55**, 857–878 (2011).
(20) N. J. Anthis and G. M. Clore, Sequence-specific determination of protein and peptide concentrations by absorbance at 205 nm, *Protein Sci.*, **22**, 851–858 (2013).
(21) X. Zhu, R. Zou, P. Sun, Q. Wang, and J. Wu, A supramolecular peptide polymer from hydrogen-bond and coordination-driven self-assembly, *Polym. Chem.*, **9**, 69–76 (2017).
(22) F. F. de Sousa, C. E. S. Nogueira, P. T. C. Freire, S. G. C. Moreira, A. M. R. Teixeira, A. S. de Menezes, J. Mendes Filho, and G. D. Saraiva, Conformational change in the C form of palmitic acid investigated by Raman spectroscopy and X-ray diffraction, *Spectrochim. Acta*, **161**, 162–169 (2016).
(23) E. Moreno-Calvo, R. Cordobilla, T. Calvet, F. Lahoz, and A. I. Balana, The C form of n-hexadecanoic acid, *Acta Crystallogr. C*, **62**, o129–o31 (2006).
(24) S. Namjoshi, I. Toth, J. Blanchfield, N. Trotter, R. Mancera, and H. E. Benson, Enhanced transdermal peptide delivery and stability by lipid conjugation: epidermal permeation, stereoselectivity and mechanistic insights, *Pharm. Res.*, **31**, 3304–3312 (2014).
(25) K. Setoh, M. Murakami, N. Araki, T. Fujita, A. Yamamoto, and S. Muranishi, Improvement of transdermal delivery of tetragastrin by lipophilic modification with fatty acids, *J. Pharm. Pharmacol.*, **47**, 808–811 (1995).
(26) J. Møss and H. Bundgaard, Prodrugs of peptides. 7. Transdermal delivery of thyrotropin-releasing hormone (TRH) via prodrugs, *Int. J. Pharm.*, **66**, 39–45 (1990).
(27) Y. L. Choi, E. J. Park, E. Kim, D. H. Na, and Y. H. Shin, Dermal stability and in vitro skin permeation of collagen pentapeptides (KTTKS and palmitoyl-KTTKS), *Biomol Ther.*, **22**, 321–327 (2014).
(28) I. W. Hamley, Self-assembly of amphiphilic peptides, *Soft Matter*, **7**, 4122–4138 (2011).
(29) A. Patist, S. S. Bhagwat, K. W. Penfield, P. Aikens, and D. O. Shah, On the measurement of critical micelle concentrations of pure and technical-grade nonionic surfactants, *J. Surfactants Deterg.*, **3**, 53–58 (2000).
(30) A. R. Bilia, L. Scalise, M. C. Bergonzi, and F. Vincieri, Effect of surfactants and solutes (glucose and NaCl) on solubility of Kavain--a technical note, *AAPS PharmSciTech*, **9**, 444–448 (2008).
(31) ProImmune, *Working with Peptides*. ProImmune Limited, 2012, accessed December 18, 2018. https://www.proimmune.com/ecommerce/pdf_files/ST55.pdf.

Purchased for the exclusive use of nofirst nolast (unknown)
From: SCC Media Library & Resource Center (library.scconline.org)